Low-velocity Impact of Sandwich Composite Plates

by J. Gustin, M. Mahinfalah, G. Nakhaie Jazar and M.R. Aagaah

ABSTRACT—In this paper we investigate impact and compression after impact properties of plain weave carbon fiber sandwich composites. Impact tests were conducted on different sample types to obtain information about absorbed energy and maximum impact force. The different samples consisted of foam-filled and hollow honeycomb cores with four-layer carbon fiber facesheets on one or both sides. The impact and compression after impact data provided valuable information to allow for comparisons between the different sample types. Also, the compression after impact tests were conducted in order to determine the reduction in compressive strength when comparing impacted to non-impacted samples. In conclusion, a two-degrees-of-freedom spring/mass model was compared to experimental results. The comparison helped illustrate the limitations of current impact theory.

KEY WORDS—Carbon fiber, composites, compression, honeycomb core, low velocity impact

Introduction

The use of woven fabrics as facesheets in composite panels is increasing due to interlacing of fiber bundles possessing high ratios of strain to failure in tension, compression or under impact loads. The core, which is typically a low strength, lightweight material, provides the distance between the facesheets required to significantly increase the overall flexural stiffness. The high stiffness, lightweight nature of the sandwich composite makes it an ideal choice for the aerospace industry. In the building construction industry, doors and some prefabricated walls are fabricated using sandwich construction.[1] The primary concern with carbon fiber sandwich composites is low and high velocity impact.[1–3] After an impact, there is a drastic reduction in compressive strength due to delamination and core damage.[4,5] While several studies have been conducted on high velocity impact, studies on low-velocity impact are of equal interest. Low-velocity impacts can include situations such as tool drops and hailstorms.

In this study, sandwich plates with different combinations of carbon fiber and cores were subjected to low-velocity impacts at energies ranging from 5 J to those that caused complete striker penetration. The low impact energy samples were considered since even in the absence of fiber breakage, the laminate mechanical performance can be drastically affected.[6] After impact, compression tests were conducted to determine the remaining compressive strength. In-plane compression is the critical load for impact-damaged specimens, since strength reductions are the largest under this type of loading.[7] The different combinations of 100×100 mm^2 samples used in this study are listed as follows:

- foam-filled (FF) honeycomb core with a four-layer carbon fiber sheet on one side (26 mm thickness, 58 g average weight) and on both sides (27 mm thickness, 75 g average weight);
- hollow honeycomb (HH) core with a four-layer carbon fiber facesheet on both sides (27 mm thickness, 41 g average weight);
- foam core (24.5 mm thickness, 42 g average weight).

Several theoretical models have been developed for sandwich composites to predict the force–time response during elastic and inelastic impacts. However, most theories do not consider the effects of facesheet cracking, which is a significant limitation. Several difficulties are present in creating accurate theoretical models. According to Ericsson and Sankar,[8] most theoretical models are based on classical sandwich plate theory, which considers the deflection of the plate and indentation of the facesheet, but neglects the deflection resulting from core compression. The deflection of the core becomes increasingly important when the deflections of the top and bottom facesheets are different. Ericsson and Sankar modeled the facesheets as laminated composite plates and the core as a three-dimensional orthotropic solid. An alternative theoretical model was used by Nemes and Simmons,[2] which utilizes a constitutive model for the facesheet and core. In addition to predicting the force–time response up to damage initiation, Hoo Fatt and Park[9] developed single-degree-of-freedom and multi-degrees-of-freedom systems to obtain the maximum force at damage initiation. They considered several damage initiation modes including tensile and shear fracture of the top facesheet, shear failure of the core, and tensile failure of the bottom facesheet. Hazizan and Cantwell[12] utilized the energy-balance method to determine the maximum forces developed during impact. They considered the energy absorbed as a result of shear/bending in addition to contact effects.

An experimental method for predicting impact response is to conduct quasi-static indentation tests, which were not considered in this study. The quasi-static load–displacement

---

This paper was presented, in part, at a symposium honoring Dr Christian P. Burger, Novel Applications of Experimental Methods in Mechanics, held at the 2003 SEM Annual Conference and Exposition on Experimental and Applied Mechanics, June 2–4, 2003, Charlotte, North Carolina.

J. Gustin (SEM member; Jeremy.Gustin@ndsu.nodak.edu) is a Graduate Student, M. Mahinfalah (SEM member) is an Associate Professor, G. N. Jazar is an Assistant Professor, and M. R. Aagaah (SEM member) is a Graduate Student, Department of Mechanical Engineering and Applied Mechanics, North Dakota State University, Fargo, ND 58105, USA.

Original manuscript submitted: October 8, 2003.
Final manuscript received: March 22, 2004.
DOI: 10.1177/0014485104046090

response is similar to low-velocity impact response.[1,3,11,12] However, Ferri and Sankar[1] mentioned that the type and the amount of damage created by the two tests are not the same. They also commented that the load and displacement levels are higher for impact tests compared to the indentation tests, which result from the dynamic effects and the viscoelastic properties of the core.

In this study, a two-degrees-of-freedom model used by Hoo Fatt and Park[13] will be considered for clamped sandwich composite plates with a linear facesheet stiffness and also negligible mass of the core. These assumptions simplified the resulting differential equation from nonlinear to linear. The theoretical results were compared to experimental data at 5 J, which is the lowest impact energy considered in the study.

The impact and compression tests were conducted in order to obtain energy, force, and compressive strength information, which can be used for comparisons. The energy and force data can be used, for example, to determine the benefits of utilizing foam core with a carbon fiber sheet on both sides compared to on one side. The compression after impact data can be used to determine how much reduction in compressive strength occurs as a result of different impact energies.

Sample Construction

A hand-layup method as shown in Fig. 1 was used to construct the samples. The major components required for this method are a vacuum pump, vacuum bagging, spiral tubing, and sealant tape. The spiral tubing ensured a uniform vacuum across the sample and prevented epoxy from pooling on the sample side with less vacuum. This would have occurred on the side without spiral tubing. When epoxy pooling occurs, the facesheet thickness is not uniform. The facesheet is the thickest on the side without the spiral tubing. The core of the sandwich composite consisted of polyurethane FF honeycomb. The honeycomb structure was constructed out of kraft paper. The FF honeycomb sheets purchased from General Plastics had the properties indicated in Table 1. Plain weave carbon fiber fabric from BGF Industries was used for this study. The carbon fiber fabric had the properties indicated in Table 2. The epoxy consisted of F-82 resin and TP-41 hardener, which was allowed to cure under a 600 mm Hg vacuum for a minimum of 9 h. The cured properties of the epoxy, purchased from Eastpointe Fiberglass, are listed in Table 3.

TABLE 1—PROPERTIES OF GENERAL PLASTICS HONEYCOMB SHEETS

Density	128 kg m^{-3}
Compressive strength	2.93 MPa
Cell size	12.7 mm
Shear strength $\perp$ to ribbon	1.88 MPa
Shear strength II to ribbon	1.58 MPa
Cell thickness	0.3175 mm
Honeycomb thickness	25.4 mm

TABLE 2—PROPERTIES OF BGF PLAIN WEAVE CARBON FIBER FABRIC

Yarn type	3 K
Area density	193 g m^{-2}
Thickness	0.3048 mm
Count (rows/tows per inch)	12.5 $\times$ 12.5

TABLE 3—PROPERTIES OF EASTPOINTE FIBERGLASS EPOXY

Density	1084 kg m^{-3}
Compressive strength	131 MPa
Tensile strength	63.6 MPa
Cure time	9–12 h
Cure temperature	75 F

The hand-layup method provided high-quality samples with minimal defects. To create the samples with the FF core, a layer of epoxy was applied before each layer of carbon fiber was placed. Special care was taken to ensure the correct amount of epoxy was used in addition to being evenly spread out. After the four layers were placed, the vacuum bagging was carefully spread over the sample, ensuring no wrinkles would form when the vacuum was applied. Any wrinkles that form on the vacuum bagging will affect the surface finish of the sample. A rubber squeegee was used to remove the extra epoxy and trapped air.

The HH core samples required three steps to construct. The first step involved creating two carbon fiber sheets with three layers each. Next, a carbon fiber layer was placed on top of the three-layer, hardened carbon fiber sheet. After the epoxy was spread out, the HH was positioned on top. A foam pad was placed on top of the HH in order to prevent the vacuum from reaching the cavities. This prevented the epoxy from pooling inside the honeycomb structure and also the carbon fiber lifting into the honeycomb structure. The other side of the sample was constructed in the same way, but the foam pad was not required since the other attached carbon fiber sheet prevented the vacuum from causing the above problems.

Test Method

An Instron Dynatup drop tower, Model 9250HV, was used for impact testing. This machine is capable of impacting samples at energies of up to 826 J utilizing a spring-assist. For this study, all samples were impacted with a 7.25 kg drop weight. Since the drop weight was not changed, the different impact energies were achieved by adjusting the drop height. A pneumatic clamping fixture, with a 76.2 mm (3 in) diameter opening, secured each sample during impact. The air pressure was set to 0.4 MPa, which was well below the 2.93 MPa compressive strength of the FF honeycomb core. The samples were impacted with a 12.7 mm (0.5 in) diameter striker, constructed out of high strength steel. Impulse software was used in order to display and store the impact data.

The compression tests were conducted using a 50 kip MTS fatigue test system. The testing fixture was designed similar to a Boeing Model No. CU-CI fixture.[14] This fixture is specifically designed to prevent buckling when compression testing thin carbon fiber facesheets. For this study, the side supports designed to prevent buckling were only used for the one-sided samples. The other samples did not fail as a result of buckling because of symmetry and thickness.

Low-Velocity Impact Results

Foam Core

The maximum force developed by the foam core was 0.96 kN at impacts of both 10 J and 20 J (Fig. 2). The maximum absorbed energy was 17.7 J and occurred at an impact of 20 J (Fig. 3). The maximum force for the 25 J impact

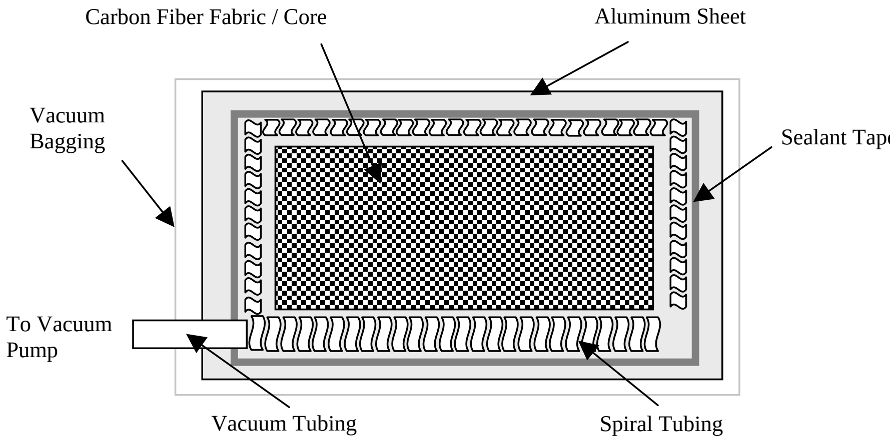

Fig. 1—Sample construction setup

was about 15% below the 20 J impact. The difference between maximum forces resulted from the honeycomb structure. When the striker impacted the honeycomb structure, higher forces and more absorbed energy were developed. However, when the striker impacted minimal honeycomb structure, it simply overcame a small shear stress and pushed out the foam. The significant difference in impact performance resulting from the striker impact location can be seen in Figs. 4(a) and (b). The diameters of the striker and the cell size were both 12.7 mm, which helps explain why the amount of honeycomb structure impacted varied substantially for the set of impacts. As a result of the non-homogeneous nature of the foam core, the force and absorbed energy results included more variation when comparing samples impacted at the same energy. This variation was larger than other sample types, which were not as dependent on the honeycomb structure.

One-Sided, FF, Four-Layer Carbon Fiber, Carbon Fiber Impacted First

The maximum force developed by the one-sided samples, carbon fiber impacted first (CFIF) was 1.65 kN at an impact of 30 J (Fig. 5). The maximum absorbed energy was 26.6 J and occurred at an impact of 30 J (Fig. 3). In general, the maximum forces for the one-sided samples, CFIF, were very close. This could be a result of the similar damage areas seen at all impact energies. With this type of impact, the carbon fiber facesheet cracked in a circular manner that corresponded to the striker diameter as can be seen in Fig. 6(a). This cracking area was consistent for all impact energies and as a result created highly localized shear stresses. In addition, the samples did not experience any noticeable delamination.

One-Sided, FF, Four-Layer Carbon Fiber, Foam Impacted First

The maximum force developed by the one-sided samples, foam impacted first (FIF), was 1.87 kN at an impact of 35 J (Fig. 7). The maximum absorbed energy was 32.9 J and occurred at an impact of 40 J (Fig. 3). There is a noticeable difference between the one-sided samples FIF and the CFIF samples. The FIF samples achieved a maximum force 13% higher and an absorbed energy 24% higher than the CFIF samples. This significant improvement results from the larger damage area experienced by the FIF samples. As the striker penetrated the foam, the drop weight was slowed and the loading was spread over a larger area on the bottom carbon fiber sheet. Since the force was applied to a larger area, more energy was required to crack and delaminate the carbon fiber facesheet. The damage area for the total penetration of the bottom carbon fiber sheet can be seen in Fig. 6(b). The delamination area cannot be seen very well, but typically had a radius between 20 and 30 mm.

Two-Sided, FF, Four-Layer Carbon Fiber (Both Sides)

The maximum force developed by the two-sided samples with a FF core was 2.16 kN at an impact of 55 J (Fig. 9). This is the largest force reached by different sample types, exceeding the one-sided carbon fiber samples, FIF and CFIF, by 15% and 31%, respectively. The maximum absorbed energy peaked at 49.5 J, which occurred at an impact of 55 J (Fig. 3). This represents a 50% increase above the one-sided samples, FIF, and an 86% increase above the one-sided samples, CFIF. A visual inspection of the damage area for the top and bottom carbon fiber sheets illustrated a significant difference. The top sheet experienced cracking corresponding to the outside diameter of the striker. However, when the striker penetrated the bottom sheet, a larger damage area with delamination occurred. This delamination area had a consistent radius between 20 and 30 mm. The damage area for the two-sided, FF samples and the one-sided, FIF samples were very similar, which is shown in Fig. 6(b). Three force–time groupings are illustrated when considering Figs. 8 and 9. Figure 8 consists of the samples where the striker penetrated the top carbon fiber sheet and slightly into the foam core, 5–20 J, and significantly into the foam core, 25–35 J. Figure 9 consists of the samples that penetrated the top carbon fiber sheet, the foam core, and either partially or fully penetrated the bottom carbon fiber sheet.

Two-Sided, HH, Four-Layer Carbon Fiber Each Side

The maximum force developed by the two-sided samples with a HH core was 1.04 kN at an impact of 15 J (Fig.10). The maximum absorbed energy was 12.1 J at an impact of 15 J (Fig. 3). The maximum force was 49% lower and maximum absorbed energy 76% lower compared to the two-sided FF samples. This is a significant reduction in impact properties

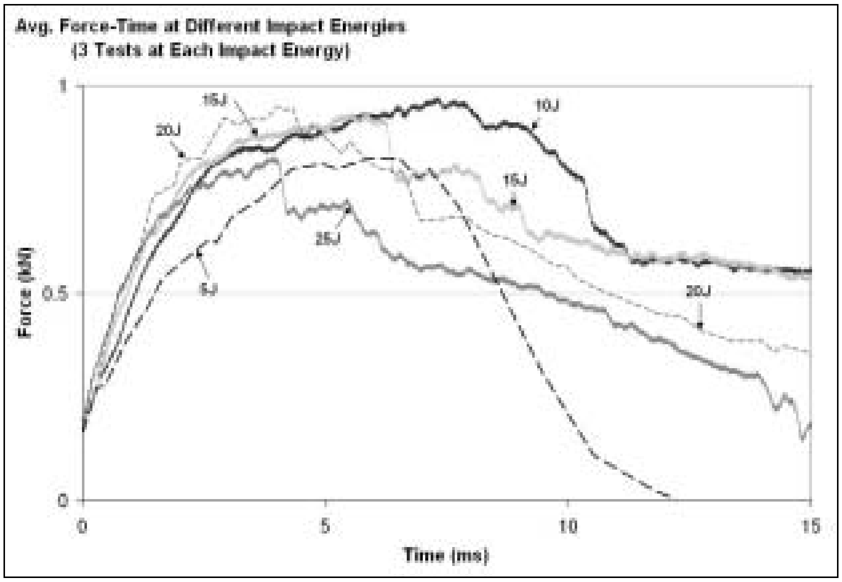

Fig. 2—Force versus time response for foam core

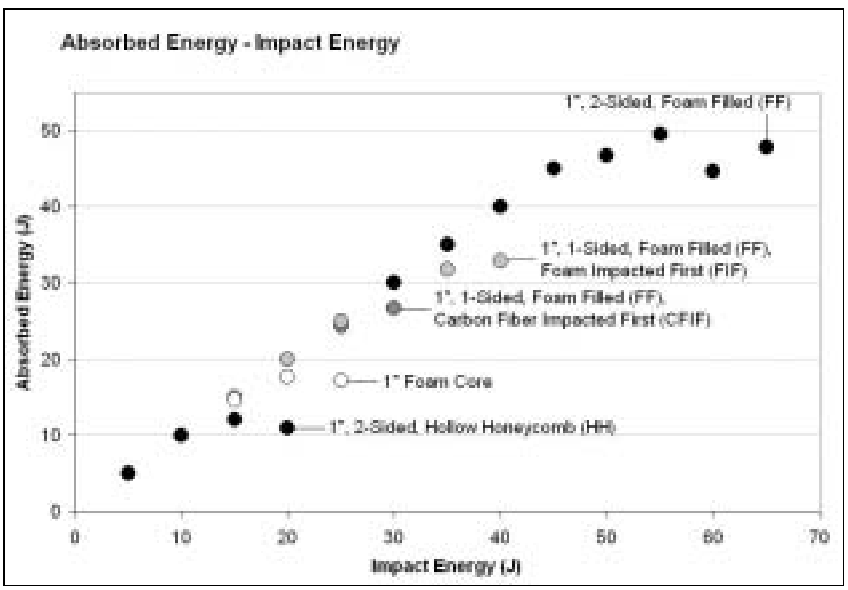

Fig. 3—Absorbed versus impact energy for all sample types

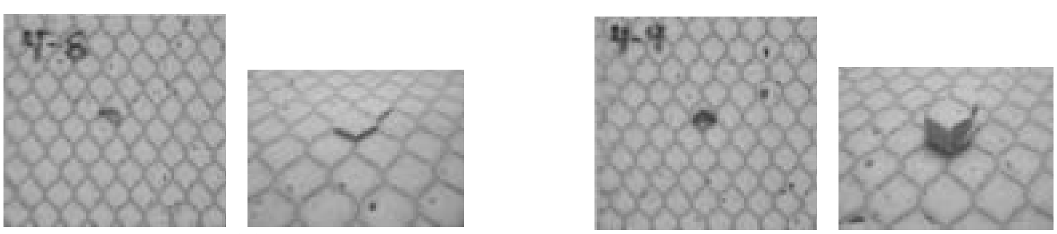

(a) (b)

Fig. 4—(a) Front and rear impact damage of FF honeycomb core where striker impacted the cell structure (10 J impact). (b) Front and rear impact damage of FF honeycomb core where striker missed the cell structure (10 J impact)

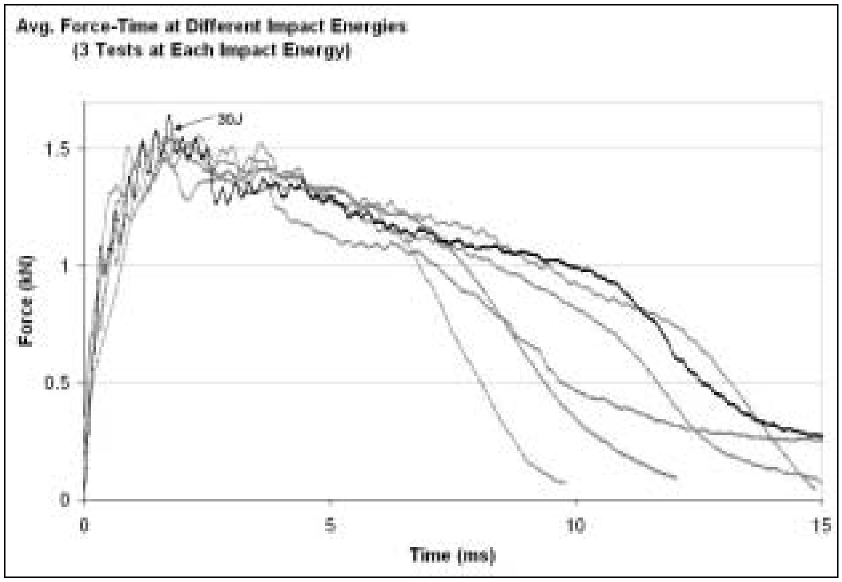

Fig. 5—Force versus time response for one-sided, FF, CFIF

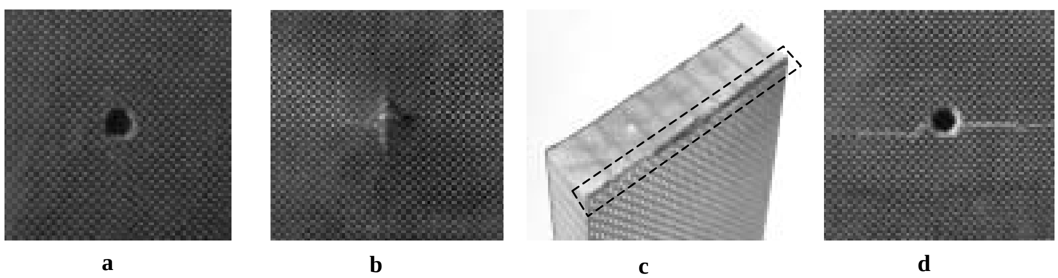

Fig. 6—(a) Front impact damage of one-sided, CFIF samples. (b) Rear impact damage of one-sided, FIF samples. (c) Facesheet cracking during compression testing of two-sided, FF samples. (d) Facesheet crushing during compression testing of two-sided, FF samples

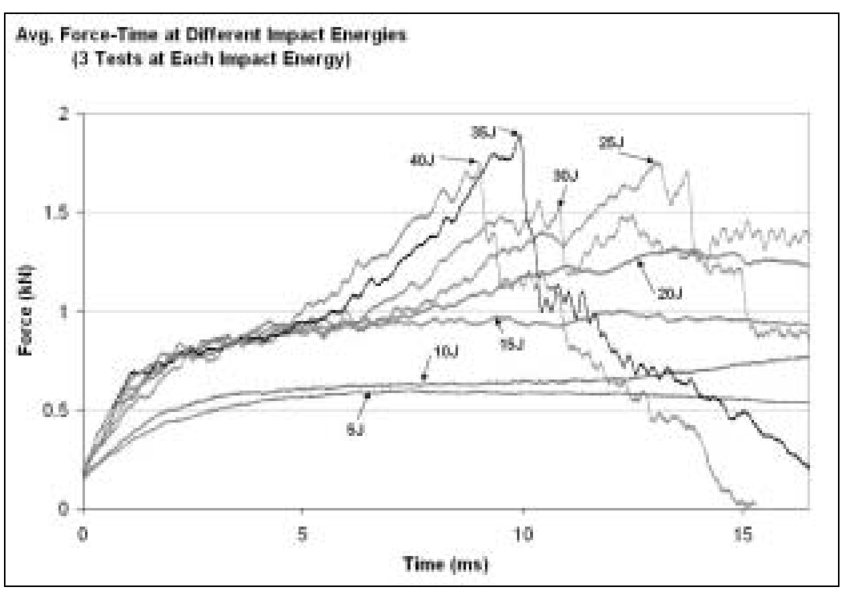

Fig. 7—Force versus time response one-sided, FF, FIF

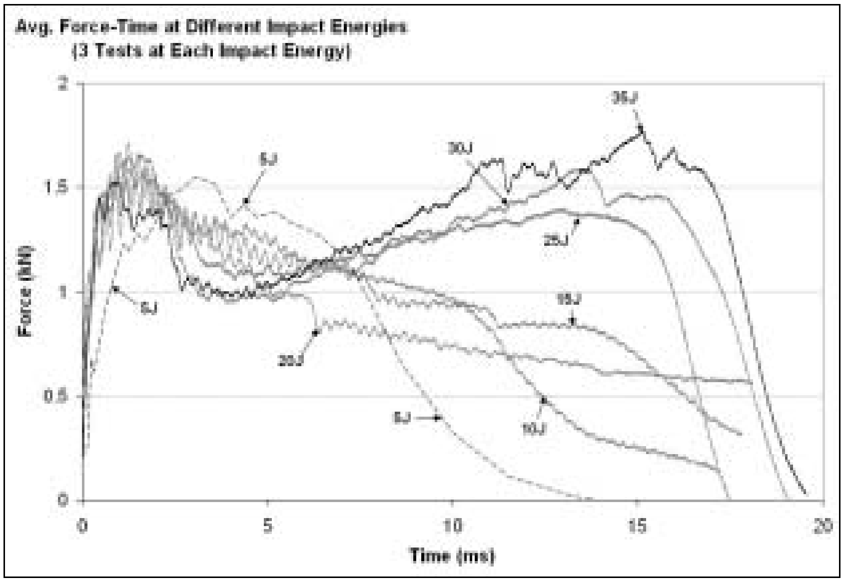

Fig. 8—Force versus time response two-sided, FF, impact energies 5–35 J

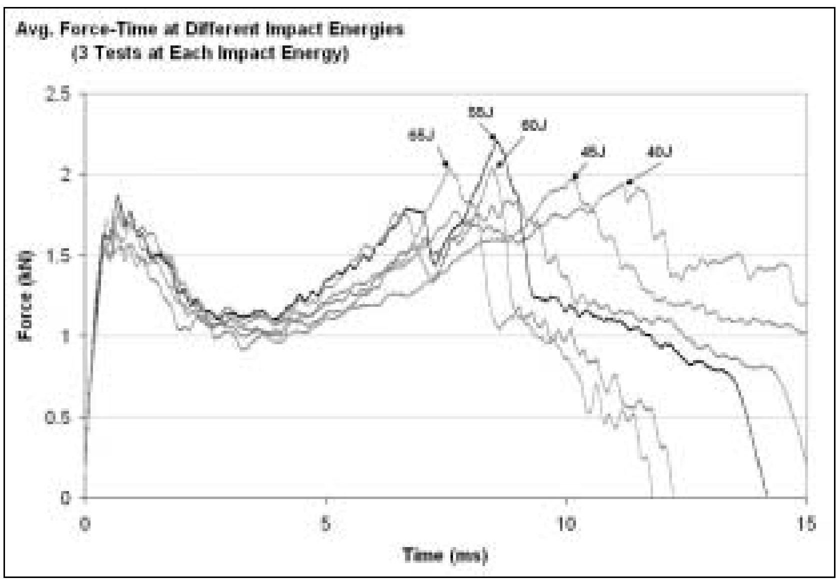

Fig. 9—Force versus time response two-sided, FF, impact energies 40–65 J

and illustrates the effectiveness of using a FF instead of HH core. A reason for the significant reduction could be the loss of bonding area between the carbon fiber sheets and the core in addition to the minimal stiffness of the HH core. The loss of bonding area significantly reduced the force required for delamination to occur. The combination of these two factors probably accounted for most of the force and absorbed energy reduction. The damage done to the top carbon fiber sheets of both the two-sided HH and FF sample types were very similar. However, a significant difference occurred between the two when the bottom carbon fiber sheet was penetrated. The bottom carbon fiber sheet of the two-sided HH samples experienced cracking at a radius only slightly larger than the top sheet, while the bottom carbon fiber sheet of the two-sided FF samples had about twice the striker radius and experienced delamination.

Compression Test Results

The maximum compressive stress, defined as compressive stress to failure, for the different sample types is shown in Fig. 11. Failure consisted of facesheet crushing, cracking, or delamination. Given this, the side supports of the Boeing CU-CI test fixture were only used on the one-sided samples, which would have otherwise experienced buckling. The side supports were not used on the other samples since the forces

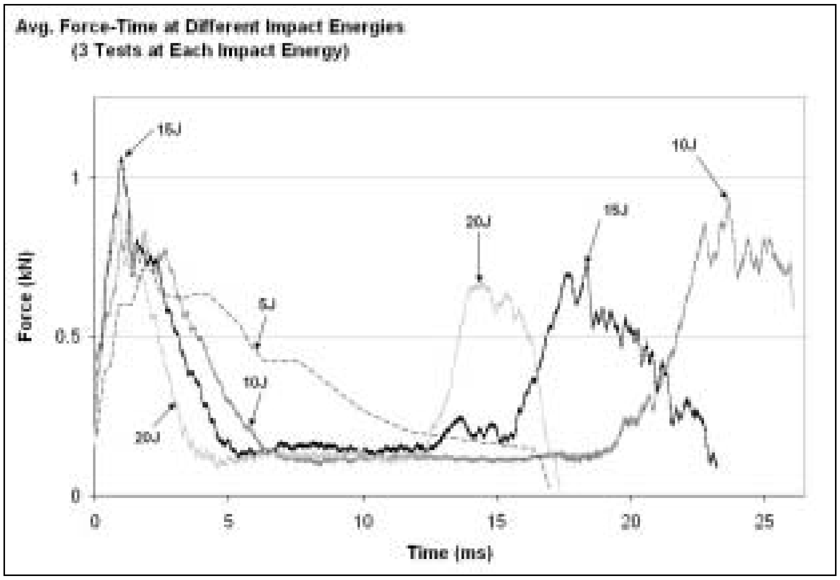

Fig. 10—Force versus time response for two-sided, HH

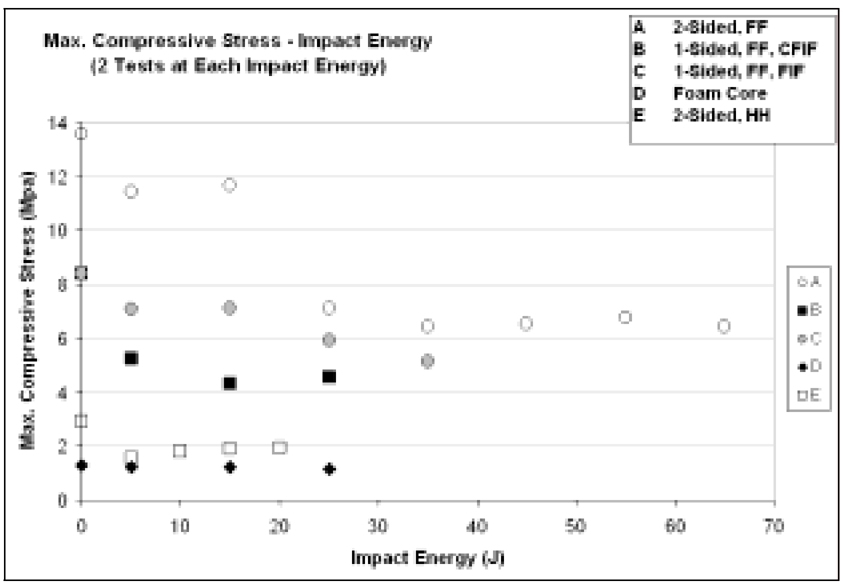

Fig. 11—Maximum compressive stress versus impact energy

required to reach facesheet delamination would have been artificially high. As can be seen, the samples followed a trend of decreasing compressive strength as impact energy increased. However, the maximum compressive strength was significantly affected depending on the type of failure that occurred. The two-sided, HH samples failed as a result of facesheet delamination. If the side supports were used, the compressive loading required to cause delamination would have been significantly higher. However, the sandwich composite cannot function properly without a strong facesheet/core bond. The minimal bonding area between the HH core and the facesheets was the primary factor causing the delamination. The facesheets of the two-sided, HH samples were capable of withstanding significantly higher compressive loads if delamination would not have occurred. The one-sided and two-sided FF samples experienced failures consisting of either facesheet crushing or facesheet cracking. The facesheet crushing occurred on samples with minimal or no initial impact damage and can be seen in Fig. 6(c). The facesheet cracking occurred from the impact hole across the sample, perpendicular to the compressive load, as can be seen in Fig. 6(d). A combination of facesheet cracking and facesheet delamination occurred on some of the one-sided, FIF samples impacted at higher energies. This likely occurred as a result of the higher energy impacts, which partially or totally penetrated the bottom facesheet. During these impacts, the bottom facesheet experienced both cracking and some delamination, which increased once the compressive load was applied.

TABLE 4—PERCENT DECREASE IN COMPRESSIVE STRENGTH

Sample Type	% Decrease
Two-sided, FF	53
One-sided, CFIF	47
One-sided, FIF	39
Foam core	12
Two-sided, HH	33

A significant difference was seen when considering the samples not impacted and those impacted at energies that caused failure, defined as total striker penetration. Table 4 presents the percentage decrease in maximum compressive strength of samples impacted at energies that caused failure compared to non-impacted samples. The overall effect of impact on compressive strength is significant for the different sample types. The greatest decrease in compressive strength due to impact occurred by the FF samples that experienced delamination. These samples included those where a carbon fiber sheet was the last layer impacted. This consisted of the two-sided, FF and the one-sided samples, FIF. The delamination originally caused by impact quickly spread when the compressive load was applied to these samples.

Theoretical Results

The following equations are used to describe the force–time response for the low-velocity impact of sandwich composite plates.[16] The equations of motion for the two-degrees-of-freedom system shown in Fig. 12 can be found using the Newtonian method, which results in

$$(M_o + M_f)(\ddot{\Delta} + \ddot{\delta}) + P_1(\delta) + Q_d = 0 \tag{1}$$

$$Q_d + P_1(\delta) = M_s\ddot{\Delta} + K_{gd}\Delta. \tag{2}$$

We assume that the inertia of the facesheet is negligible compared to that of the impactor. Also, we assume that the local spring response can be linearized

$$P_1(\delta) \approx K_{ld}\delta. \tag{3}$$

Therefore, eqs (1) and (2) reduce to

$$M_o(\ddot{\Delta} + \ddot{\delta}) + K_{ld}\delta + Q_d = 0 \tag{4}$$

$$Q_d + K_{ld}\delta = K_{gd}\Delta. \tag{5}$$

Differentiating eq (5) twice with respect to time t results in

$$\ddot{\Delta} = \frac{K_{ld}}{K_{gd}}\ddot{\delta}. \tag{6}$$

Substituting eq (6) into eq (4) we obtain

$$M_o\left(1 + \frac{K_{ld}}{K_{gd}}\right)\ddot{\delta} + K_{ld}\delta + Q_d = 0. \tag{7}$$

Equation (7) is subject to the initial conditions

$$\dot{\delta}(0) = \delta_o = \frac{K_{gd}V_o}{(K_{gd} + K_{ld})}, \delta(0) = 0.$$

The solution for δ gives

$$\delta = \frac{\dot{\delta}_o}{\omega}\sin\omega t + \frac{Q_d}{K_{ld}}\cos\omega t - \frac{Q_d}{K_{ld}}, \tag{8}$$

where

$$\omega = \sqrt{\frac{K_{ld}K_{gd}}{(K_{ld} + K_{gd})M_o}}.$$

The impact force as a function of time is given by

$$F(t) = -M_o(\ddot{\Delta} + \ddot{\delta}) = -M_o\left(1 + \frac{K_{ld}}{K_{gd}}\right)\ddot{\delta} \tag{9}$$

or

$$F(t) = M_o\left(1 + \frac{K_{ld}}{K_{gd}}\right)\left(\omega\dot{\delta}_o\sin\omega t + \frac{Q_d\omega^2}{K_{ld}}\cos\omega t\right). \tag{10}$$

The theoretical force–time response at 5 J, the lowest impact energy considered in this study, was compared to experimental results in order to show the limitations of current theory when considering high-mass, low-velocity impacts. The two-sided, FF samples were used for the comparison. The results are expected to vary from theoretical results, which are useful for impacts without facesheet cracking.

The static core crushing strength, q, was found using ASTM standard C365.[18] The total dynamic core crushing strength was assumed the same as the dynamic core crushing strength, q_d. Actually, the total dynamic core crushing strength is higher than static. However, this simplification had a minimal lowering effect on the theoretical results, which would have compared even worse to experimental if the true dynamic core crushing strength was used. The total dynamic core crushing strength is given by

$$Q_d = \pi R^2 q_d \tag{11}$$

where R is the radius of the striker. The static core crushing strength was 1.94 MPa for the FF honeycomb core.

The local and total dynamic stiffness values were determined experimentally for the 5 J impact. The total dynamic stiffness includes the deflection that results from local damage and also the bending of the sandwich composite plate during impact. To find total dynamic stiffness, the force and deflection data already obtained from the two-sided, FF impact were used. The local dynamic stiffness was found by placing a steel plate underneath the sandwich composite sample in order to prevent bending during impact. The local and total stiffness values were approximated by taking the slope of the force–deflection curve before facesheet cracking occurred. For the 5 J impact, the maximum deflection for the linear portion was approximately 1.8 mm. The global stiffness was determined using the relationship for springs in series as follows:

$$K_{tot} = \frac{K_{ld}K_{gd}}{K_{ld} + K_{gd}}. \tag{12}$$

The local stiffness and total stiffness were 0.96 and 0.79 kN m^{-1}, respectively. Therefore, the resulting global stiffness was 4.57 kN m^{-1}.

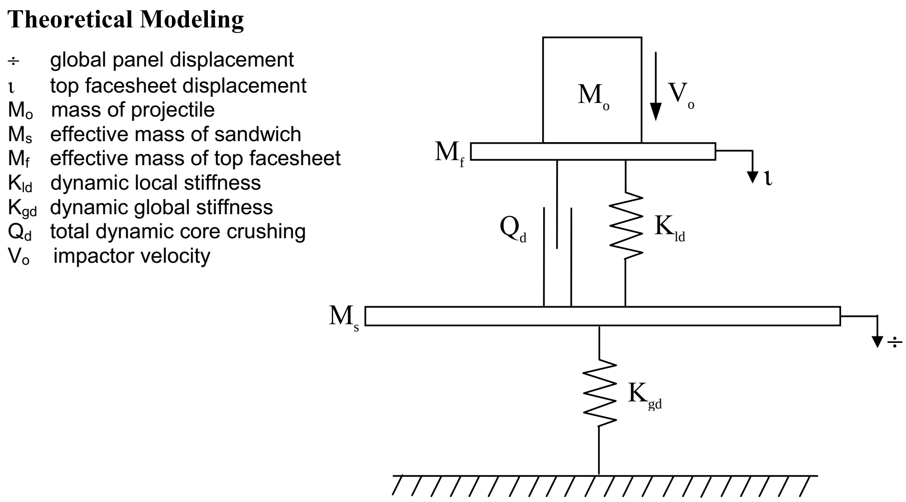

Fig. 12—Clamped panel model for low-velocity impact

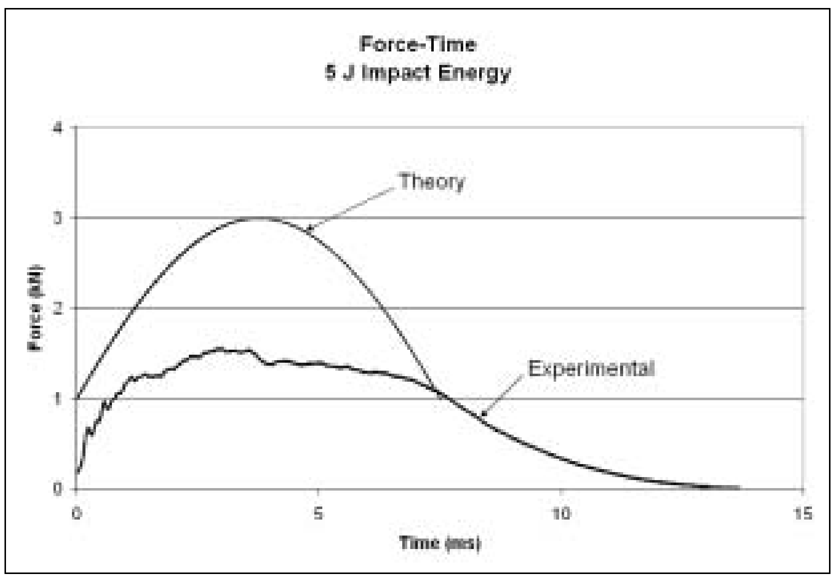

Fig. 13—Force versus time response for two-sided, FF 5 J impact

Two-Sided, FF, Four-Layer Carbon Fiber (Both Sides)

The theoretical and experimental results at 5 J varied as can be seen in Fig. 13. The maximum experimental impact force for the 5 J impact was 50% lower than the theoretical prediction. The large difference between theory and experiment was likely due to the facesheet cracking that occurred at the 5 J impact. To better compare theoretical results to experimental impact tests much lower than 5 J should be considered, but this is below the 9250HV drop tower capability. Also, more layers could have been added to the facesheet, but this was not considered because samples with four-layer facesheets were the focus of this study. Given that impacts involving facesheet cracking are of interest for determining applications for sandwich composites, experimental studies must continue.

Conclusion

The information obtained from the impact and compression after impact tests was used to identify trends and make comparisons. Significant differences in impact properties occurred for the different sample types. The two-sided, FF samples performed best considering both impact and compression after impact testing. These samples were able to absorb a maximum of 49.5 J and withstand a compressive stress above 6 MPa, even after being impacted at energies that caused complete striker penetration. These values are significantly higher than all other sample types. The two-sided, HH samples performed considerably worse than the two-sided, FF samples and both one-sided foam impacted first and one-sided carbon fiber impacted first. The significant reduction in impact properties was primarily due to the poor stiffness and small bonding area.

The theoretical and experimental results varied at 5 J. The maximum experimental forces for the 5 J impact was 50% lower than theoretical. This resulted from extensive facesheet cracking that occurred at the 5 J impact, which helps illustrate the limitations of current impact theory. Experimental impact testing of sandwich composites must continue to be researched in order to determine the impact performance for a wide range of impact energies, including those that cause facesheet cracking.

Acknowledgments

The National Science Foundation, under Grant 0082832, and the NASA Space Grant Fellowship Program provided funding for this research. Their support is greatly appreciated.

References

1. Ferri, R. and Sankar, B.V., "Static Indentation and Low-Velocity Impact Tests on Sandwich Plates," ASME, **55***, 485–490 (1997).*

2. Nemes, J.A. and Simmonds, K.E., "Low-Velocity Impact Response of Foam-Core Sandwich Composites," Journal of Composite Materials, **26***, 501–519 (1992).*

3. Williamson, J.E. and Lagace, P.A., "Response Mechanisms in the Impact of Graphite/Epoxy of Graphite/Epoxy Honeycomb Sandwich Panels," Proceedings of the American Society for Composites 8th Technical Conference: Composite Materials, Cleveland, OH, 287–296 (1993).

4. Vaidya, U.K., "Impact Response of Integrated Hollow Core Sandwich Composite Panels," Composites A, **31***, 761–772 (2000).*

5. Kim, W.C. and Dharan, C.K.H, "Facesheet Debonding Criteria for Composite Sandwich Panels Under In-Plane Compression," Fracture Mechanics, **42***, 643–652 (1992).*

6. Lee, M.L., "Instrumented Impact and Static Indentation of Composites," Composite Materials, **25***, 204–222 (1991).*

7. Abrate, S., "Impact on Laminate Composites: Recent Advances," Applied Mechanics Review, **47***, 517–544 (1998).*

8. Ericsson, A. and Sankar, B.V., "Contact Stiffness of Sandwich Plates and Application to Impact Problems," Proceedings of Sandwich Construction 2, Part 1, UK:EMAS, 139–159 (1992).

9. Hoo Fatt, M.S. and Park, K.S., "Dynamic Models for Low-Velocity Impact Damage of Composite Sandwich Panels—Part B: Damage Initiation," Composite Structures, **52***, 353–364 (2001).*

10. Hazizan, A. and Cantwell, W.J., "The Low-Velocity Impact Response of Foam-Based Sandwich Structures," Composites Part B: Engineering, **33***, 193–204 (2002).*

11. Herup, E.J. and Palazotto, A.N., "Low-Velocity Impact Damage Initiation in Graphite/Epoxy/Nomex Honeycomb-Sandwich," Composites Science and Technology, **57***, 1581–1598 (1997).*

12. Soden, P.D. and Shuaeib, F.M., "Indentation Failure of Composite Sandwich Beams," Composites Science and Technology, **57***, 1249–1259 (1997).*

13. Hoo Fatt, M.S. and Park, K.S., "Dynamic Models for Low-Velocity Impact Damage of Composite Sandwich Panels—Part A, Deformation," Composite Structures, **52***, 335–351 (2001).*

14. Boeing Compression After Impact Test Fixture. Wyoming Test Fixture Inc., http://www.wyomingtestfixtures.com/Products/page26-27.htm.

15. "Standard Test Methods for Flatwise Compressive Strength of Sandwich Cores," ASTM Standards and Literature References for Composite Materials, ASTM, Philadelphia, PA (1990).